



# Measurements of octanol–air partition coefficients, vapor pressures and vaporization enthalpies of the (E) and (Z) isomers of the 2-ethylhexyl 4-methoxycinnamate as parameters of environmental impact assessment



César N. Pegoraro<sup>a</sup>, Malisa S. Chiappero<sup>a,\*</sup>, Hernán A. Montejano<sup>b</sup>

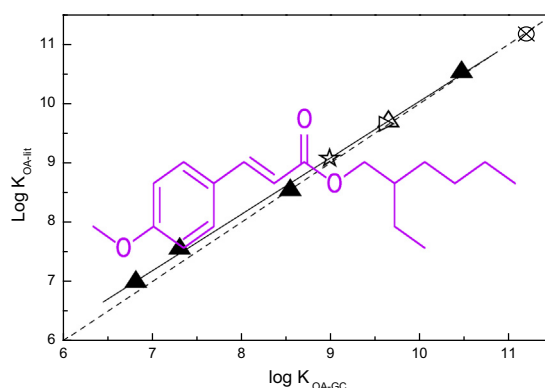
<sup>a</sup>Departamento de Química, Facultad de Ciencias Exactas y Naturales, Universidad Nacional de Mar del Plata, Funes 3350, 7600 Mar del Plata, Argentina

<sup>b</sup>Departamento de Química, Facultad de Ciencias Exactas, Físico-Químicas y Naturales, Universidad Nacional de Río Cuarto, 5800 Río Cuarto, Argentina

## HIGHLIGHTS

- Z-EHMC is around 5 times more volatile than E-EHMC isomer.
- E- and Z-EHMC are substances with a relatively low mobility ( $8 < \log K_{OA} < 10$  and  $-4 < \log(P_L/Pa) < -2$ ).
- A  $\log K_{OA} = 9.12 \pm 0.56$  and  $11.18 \pm 0.71$  were obtained for BBP and DOP, respectively.
- For BBP, E- and Z-EHMC are expected to have low particle-bound.

## GRAPHICAL ABSTRACT



## ARTICLE INFO

### Article history:

Received 21 April 2015

Received in revised form 8 July 2015

Accepted 13 July 2015

### Keywords:

E-EHMC

Z-EHMC

Phthalate

UV filters

Chemical mobility

Environmental impact

## ABSTRACT

2-Ethylhexyl 4-methoxycinnamate is one of the UVB blocking agents more widely used in a variety of industrial fields. There are more than one hundred industrial suppliers worldwide. Given the enormous annual consumption of octinoxate, problems that arise due to the accumulation of this compound in nature should be taken into consideration. The GC-RT was used in this work with the aim of determining the vapor pressure, enthalpies of vaporization and octanol–air partition coefficient, for the BBP, DOP, E- and Z-EHMC esters. The results showed that Z-EHMC is almost five times more volatile than E-EHMC. Moreover, BBP, Z-EHMC and E-EHMC can be classified as substances with a relatively low mobility since they lie within the range of  $8 < \log K_{OA} < 10$  and  $-4 < \log(P_L/Pa) < -2$ , while DOP lies in the range of  $\log K_{OA} > 10$  and  $\log(P_L/Pa) < -4$ , therefore, a low mobility can be expected. From these parameters, their particle-bound fraction and gas–particle partition coefficient were also derived.

© 2015 Elsevier Ltd. All rights reserved.

## 1. Introduction

UV filters emerge as environmental pollutants and constitute a heterogeneous group of chemicals that are found in personal care

\* Corresponding author.

E-mail address: [mchiappero@mdp.edu.ar](mailto:mchiappero@mdp.edu.ar) (M.S. Chiappero).

products, mainly, to protect the body from sunlight. Moreover, they are used in industrial products such as paints, pesticides, plastics, or textiles in order to prevent the photodegradation of their components (Richardson, 2010; Zenker et al., 2008).

The 2-ethylhexyl 4-methoxycinnamate (EHMC or octinoxate) is one of the most commonly used chemical UV filters. It has been detected in untreated and treated waste waters (Balmer et al.,

### Nomenclature

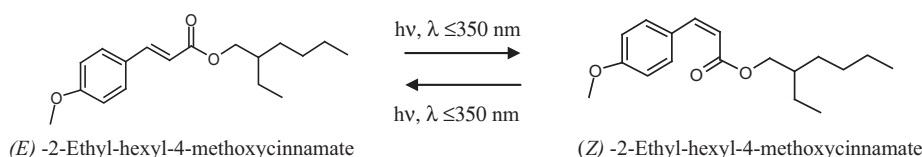
GC	gas chromatography	DMP	dimethyl phthalate
GC-RT	gas chromatographic retention time methodology	DEP	diethyl phthalate
$t_M$	holdup time	DBP	dibutyl phthalate
$t_a$	adjusted retention time	BBP	bencyl butyl phthalate
$\Delta H_{trn}$	enthalpy of transfer	DOP	di-n-octyl phthalate
$\Delta H_{intr}$	enthalpy of interaction of the analyte with the column	DEHP	bis (2-ethylhexyl) phthalate
$\Delta H_{vap}(T_{298})$	enthalpy of vaporization at 298.15 K	$K_{OA}$	octanol–air partition coefficient
$T_m$	mean temperature	$P_L$	liquid vapor pressure
PAHs	polycyclic aromatic hydrocarbons	TSP	total suspended particulate matter
E-EHMC	E-2-ethylhexyl 4-methoxycinnamate	SVOCs	semi-volatile organic compounds
Z-EHMC	Z-2-ethylhexyl 4-methoxycinnamate	$K_p$	gas–particle partition coefficient
EHMCs	E and Z-2-ethylhexyl 4-methoxycinnamate	$\Phi$	fraction of substance associated with the particle phase in air
FAME 16:0	methyl hexadecanoate	PM <sub>2.5</sub>	particulate matter (2.5 $\mu\text{m}$ )
FAME 18:0	methyl octadecanoate		
HCBz	hexachlorobenzene		

2005; Magi et al., 2013), surface waters (Giokas et al., 2005) and in organic aerosols (Mayol-Bracero et al., 2001). In aquatic environments, bioaccumulation was detected in a trophic network involving fish and birds (Fent et al., 2010). In addition, possible endocrine activity could imply a potential risk to human health (Schlumpf et al., 2008).

The exposition of EHMC to the UV radiation produces an isomerization in the double bond and consequently two photoisomers can exist, as (Z) or (E). Commercial sunscreens are composed only of E-EHMC isomer but, in the case of the other formulations, it is possible to find one or both isomers. Nevertheless, the solar UV radiation can generate both isomers within the environment (Pattanaarjson et al., 2004; MacManus-Spencer et al., 2011). See Scheme 1.

In order to explain the fate of these substances within the environment, it is essential to know their physico-chemical properties. Particularly, their atmospheric fate requires quantitative information regarding about their partition into atmospheric particles, aerosols and water droplets, as well as their volatility. Several parameters have been used to express the volatility of organic chemicals, of which:  $P_L$  indicates the tendency of a chemical to volatilize, whereas  $K_{OA}$  describes the equilibrium partitioning of a chemical between pure organic solvent and the gas phase in contact. All these parameters are strongly influenced by temperature.  $K_{OA}$  is a useful descriptor of chemical mobility in the atmospheric environment and it can be used to calculate the absorptive partitioning of the semi-volatile compounds between the atmosphere and organic phases found in soil (Odabasi and Cetin, 2012), in vegetation (Wania and McLachlan, 2001), and in aerosols (Radonic et al., 2011).

This study reports ( $P_L/\text{Pa}$ ),  $K_{OA}$  and  $\Delta H_{vap}$  ( $\text{kJ mol}^{-1}$ ) measurements, for the E and Z-EHMC isomers as a function of temperature, using the GC-RT. Also, a revision of the  $K_{OA}$  values for BBP and DOP are reported. Also their particle-bound fraction,  $\Phi/\%$ , and gas–particle partition coefficient,  $K_p$  were estimated.



Scheme 1. Photoisomerization.

## 2. Experimental section

### 2.1. Experimental methodology

*Comment:* For abbreviations and symbols meanings used in this text, refer to nomenclature section.

GC-RT was used to determine the  $P_L$  and  $K_{OA}$  of the substances under study (Bidleman, 1984; Chickos et al., 2004; Wania et al., 2002; Odabasi et al., 2006). It has been strongly established that the analyte vapor pressure governs its movement along the column and the amount of time that each analyte spends on the chromatographic column,  $t_a$ , should be inversely proportional to its vapor pressure. Using a  $t_0 = 60$  s as a reference time and plotting  $\ln(t_0/t_a)$  against  $1/T$  for each analyte, the results show a straight line. When its slope is multiplied by  $R$  ( $\text{kJ mol}^{-1} \text{K}^{-1}$ ), it results in the enthalpy of transfer,  $-\Delta H_{trn}(T_m)$ , of each analyte from the column's stationary phase to the gas carrier (Chickos and Lipkind, 2010).

$$\Delta H_{trn}(T_m) = \Delta H_{vap}(T_m) + \Delta H_{intr}(T_m) \quad (1)$$

The  $\Delta H_{vap}(T_{298})$  for the target substance can be evaluated from the correlation equation between  $\Delta H_{trn}(T_m)$  and the literature  $\Delta H_{vap}(T_{298})$ . The selection of reference substances is usually influenced by the nature of the functional groups involved and lesser so by the hydrocarbon structural portion of the molecule. Usually, the best results are obtained when the structure of the references closely resembles the structure of the target substances.

A linear behavior was obtained by plotting parameter of Eq. (2) at each temperature.

$$\ln(t_{R,i}/t_{R,ref}) = (\Delta_{OA}U_i/\Delta_{OA}U_{ref}) \ln K_{OA,ref} + C \quad (2)$$

Using the slope of Eq. (2), the volatilization energy ratio between the target and reference substances can be estimated. Furthermore, this ratio, consequently, can be used to calculate the uncalibrated octanol–air partition coefficients ( $K_{OA-GC}$ ) using

$$\ln(K_{\text{OA-GC}}) = (\Delta_{\text{OA}}U_i / \Delta_{\text{OA}}U_{\text{ref}}) \ln(K_{\text{OA,ref}}) + c \quad (3)$$

The  $K_{\text{OA-GC}}$  values are not necessarily identical to  $K_{\text{OA}}$  and they were converted into  $K_{\text{OA-cal}}$  using a number of calibration compounds for which  $K_{\text{OA}}$  are well known from techniques other than the GC-RT used in this work. Previous studies relying on the GC-RT had successfully employed reference compounds that are quite different from the target substances (Hinckley et al., 1990). In this work, hexachlorobenzene (HCBz) served as a reference compound in  $K_{\text{OA-GC}}$  determinations because its  $K_{\text{OA}}$  is well established as a function of temperature (Shoeib and Harner, 2002).

GC-RT is a widespread technique applied in determination of vaporization properties of organic substances and trusted for the rapidness, robustness, and reliability of its measurements and requiring low levels of purity for the samples. Nevertheless, experimental vaporization properties reliability and the standards selection affect directly the results (Chickos et al., 1995).

## 2.2. Materials

n-Hexane chromatographic grade (purity > 98.5%). E-EHMC (purity > 99.5%). The analyte Z-EHMC was obtained by UV Photolysis ( $\lambda = 254 \text{ nm}$ ) of an E-EHMC solution in n-hexane, its purity was checked by HPLC-UV-vis (KONIC-KNK-500). The FAMES 16:0 and 18:0 present in the FAMES-001-R1-KIT MIX (purity 99%) were used as mono-ester control substances. A standard solution M-8270-01-ASL (purity 99%) containing DMP, DEP, DBP, BBP, DEHP, DOP and HCBz were used as reference substances.

## 2.3. Experimental set-up

All compounds were analyzed as mixtures in a Shimadzu GCMS-QP2100ULTRA-AOC20i using an injector at 553 K with a 10/1 split ratio, a column of 25 mm ID, 30 m and 0.1 mm phase thickness Zebron ZB-5MS. The oven temperature in each isothermal method was kept within  $\pm 0.1 \text{ K}$ . Helium chromatographic grade (99.9999%) was used as the carrier gas with a constant linear velocity of  $35.2 \text{ cm s}^{-1}$ .

The interface and the ionization source were kept at 553 K and 473 K, respectively. Electron impact ionization was used at 70 eV and ions from 50 to 700 amu were recorded in a scan mode. The references were injected simultaneously with the target substances using a non-retained analyte.

Experimental adjusted retention time ( $t_a = t - t_M$ ) of the target and reference substances were obtained. The holdup time,  $t_M$ , was determined in a selected ion monitoring mode (SIM), at all temperatures, from the nitrogen peak of injected air. The adjusted retention time,  $t_a$ , was measured over a temperature range of around 70 K at 5 K intervals. The uncertainties reported in the final column of Tables 1–3 were calculated taking into account the uncertainty in the slope and intercept of the equations listed at the bottom of each respective table.

## 3. Results and discussion

The phthalates were used as reference compounds of the E-EHMC and Z-EHMC esters. In order to support the good behavior of these references, the well characterized FAMES 16:0 and 18:0 were also measured and used as control substances together with BBP and DOP.

### 3.1. Estimation of the vaporization enthalpies

Table 1, collects the results of the  $\Delta H_{\text{trn}}(T_m)$ , obtained from the slope, using the correlations of  $\ln(t_0/t_a)$  vs  $1/T$  for all the compounds measured (see supplementary information S1).

In the majority of cases, the vaporization enthalpy data available from literature are reported as  $\Delta H_{\text{vap}}(T_{298})$  but, in these experiments, the  $\Delta H_{\text{trn}}(T_m)$  were obtained.  $T_m$  is bigger than 298.15 K, generally. So, it is necessary to correlate the experimental  $\Delta H_{\text{trn}}(T_m)$  data against the  $\Delta H_{\text{vap}}(T_{298})$  from the literature. As it can be seen in Figure N° S2.1 (supplementary information S.2) a linear relationship was obtained for the phthalates and also provides a visual assessment of the correlation quality.

Regarding E- and Z-EHMC there are not any experimental values of  $\Delta H_{\text{vap}}(T_{298})$  reported in literature for comparison. The experimental  $\Delta H_{\text{vap}}(T_{298}) = 105.00 \pm 1.80 \text{ kJ mol}^{-1}$  for BBP agrees, within experimental error, with the value reported by Gobble et al. (2014). In the case of DOP, a  $\Delta H_{\text{vap}}(T_{298}) = 126.56 \pm 2.01 \text{ kJ mol}^{-1}$  is within the range of the values 122.6 and 130.4  $\text{kJ mol}^{-1}$  determined by Gobble et al. (2014) and Perry and Weber (1949), respectively.

A  $\Delta H_{\text{vap}}(T_{298}) = (108.91 \pm 1.82) \text{ kJ mol}^{-1}$  was measured for E-EHMC which is substantially different from the estimated value of  $65.7 \pm 3.0 \text{ kJ mol}^{-1}$  at boiling point, using the ACD Laboratories

**Table 1**  
Results of the correlations obtained between enthalpies of transfer measured from  $\ln(t_0/t_a)$  vs  $1/T$  plots and literature vaporization enthalpies.

	Slope <sup>a</sup> T/K	Intercept <sup>a</sup>	$\Delta H_{\text{trn}}(T_m)$ kJ mol <sup>-1</sup>	$\Delta H_{\text{vap}}(298 \text{ K})$ (lit) kJ mol <sup>-1</sup>	$\Delta H_{\text{vap}}(298 \text{ K})$ (calcd) <sup>k</sup> kJ mol <sup>-1</sup>
DMP	-6627 ± 40	14.16 ± 0.10	55.07 ± 0.43	77 <sup>b</sup>	76.93 ± 1.54
DEP	-7087 ± 45	14.61 ± 0.19	59.04 ± 0.83	82.1 <sup>c</sup>	82.36 ± 1.59
DBP	-8303 ± 56	16.11 ± 0.16	70.15 ± 0.75	96 <sup>d</sup>	95.71 ± 1.72
Z-EHMC	-8596 ± 50	15.39 ± 0.13	70.30 ± 0.65	-	98.93 ± 1.75
BBP	-9149 ± 50	14.31 ± 0.16	68.26 ± 0.83	106.5 <sup>e</sup>	105.00 ± 1.80
FAME 16:0	-8317 ± 45	15.60 ± 0.10	69.11 ± 0.37	96.8 <sup>f</sup> -96.16 <sup>g</sup>	95.86 ± 1.72
FAME 18:0	-9152 ± 45	17.05 ± 0.10	76.05 ± 0.37	105.9 <sup>f</sup> -106.1 <sup>g</sup>	105.03 ± 1.80
E-EHMC	-9323 ± 58	16.53 ± 0.14	76.83 ± 0.67	-	108.91 ± 1.82
DEHP	-10223 ± 46	17.83 ± 0.10	84.95 ± 0.38	116.7 <sup>h</sup>	116.80 ± 1.92
DOP	-11112 ± 62	19.15 ± 0.13	92.34 ± 0.52	122.6 <sup>c</sup> -130.4 <sup>i</sup>	126.56 ± 2.01

<sup>a</sup> The slope and intercept of the line obtained by plotting  $\ln(t_0/t_a)$  against  $1/T$ .

<sup>b</sup> Mackay et al. (2006).

<sup>c</sup> Small et al. (1948).

<sup>d</sup> Stephenson and Malanowski (1987).

<sup>e</sup> Gobble et al. (2014).

<sup>f</sup> van Genderen et al. (2002).

<sup>g</sup> Chickos et al. (2004).

<sup>h</sup> EPA (2015a,b).

<sup>i</sup> Perry and Weber (1949).

<sup>k</sup> This work.

**Table 2**  
Correlation of  $\ln(t_0/t_a)$  with experimental  $\ln(P_L/\text{Pa})$  values at  $T/K = 298.15$ .<sup>a</sup>

	Slope $T/K$	Intercept	$\ln(t_0/t_a)$	$\ln(P_L/\text{Pa})_{\text{lit}}$	$\ln(P_L/\text{Pa})_{\text{calcd}}$
DMP	$-6627 \pm 40$	$14.16 \pm 0.10$	$-8.04 \pm 0.19$	$-1.204^{\text{b}}$	$-1.071 \pm 0.082$
DEP	$-7087 \pm 45$	$14.61 \pm 0.19$	$-9.19 \pm 0.26$	$-2.313^{\text{c}}$	$-2.411 \pm 0.058$
DBP	$-8303 \pm 56$	$16.11 \pm 0.16$	$-12.05 \pm 0.32$	$-5.627^{\text{d}}$	$-5.712 \pm 0.003$
Z-EHMC	$-8596 \pm 50$	$15.39 \pm 0.13$	$-13.15 \pm 0.27$	–	$-6.987 \pm 0.027$
BBP	$-9149 \pm 50$	$14.31 \pm 0.16$	$-14.45 \pm 0.47$	$-6.812^{\text{e}}$	$-8.484 \pm 0.054$
FAME-C16	$-8317 \pm 45$	$15.60 \pm 0.10$	$-11.90 \pm 0.25$	$-5.073^{\text{f}}$	$-5.537 \pm 0.001$
FAME-C18	$-9152 \pm 45$	$17.05 \pm 0.10$	$-13.65 \pm 0.25$	$-7.331^{\text{f}}$	$-7.564 \pm 0.037$
E-EHMC	$-9323 \pm 58$	$16.53 \pm 0.14$	$-14.57 \pm 0.32$	–	$-8.626 \pm 0.057$
DEHP	$-10223 \pm 46$	$17.83 \pm 0.10$	$-16.46 \pm 0.26$	$-10.87^{\text{g}}$	$-10.814 \pm 0.097$
DOP	$-11112 \pm 62$	$19.15 \pm 0.13$	$-16.57 \pm 0.32$	$-12.11^{\text{e}}$	$-12.737 \pm 0.132$

<sup>a</sup> Eq. (5).

<sup>b</sup> Rohac et al. (1999).

<sup>c</sup> Rohac et al. (2004).

<sup>d</sup> Staples et al. (1997).

<sup>e</sup> Gobble et al. (2014), Clausen et al. (2002) and Gobble et al. (2014).

<sup>f</sup> van Genderen et al. (2002) and Chickos et al. (2004).

<sup>g</sup> Clausen et al. (2002).

**Table 3**  
Octanol–air partition coefficients determined by GC-RT: Uncalibrated ( $K_{\text{OA-CC}}$ ), calibrated ( $K_{\text{OA-cal}}$ ) and literature ( $K_{\text{OA-lit}}$ ) for selected phthalates, E-EHMC and Z-EHMC at 298.15 K.

Compound	$\log K_{\text{OA-CC}}$	Slope	Intercept	$\Delta_{\text{OA}}U/\text{kJ mol}^{-1}$	$\log K_{\text{OA-lit}}^{\text{a}}$	$\log K_{\text{OA-cal}}$
DMP	$6.80 \pm 0.19$	$6611 \pm 33$	$-6.50 \pm 0.08$	$126.52 \pm 0.63$	7.0	$7.00 \pm 0.55$
DEP	$7.31 \pm 0.26$	$7107 \pm 46$	$-7.01 \pm 0.11$	$136.01 \pm 0.88$	7.5	$7.48 \pm 0.57$
DBP	$8.55 \pm 0.32$	$8326 \pm 56$	$-8.22 \pm 0.13$	$159.34 \pm 1.07$	8.5	$8.66 \pm 0.61$
Z-EHMC	$8.99 \pm 0.33$	$8543 \pm 61$	$-7.95 \pm 0.13$	$163.49 \pm 1.17$	–	$9.08 \pm 0.63$
BBP	$9.60 \pm 0.28$	$9174 \pm 50$	$-8.67 \pm 0.11$	$175.57 \pm 0.96$	8.7	$9.66 \pm 0.31$
E-EHMC	$9.65 \pm 0.32$	$9346 \pm 58$	$-9.13 \pm 0.13$	$178.86 \pm 1.11$	$9.93^{\text{b}}$	$9.70 \pm 0.66$
DEHP	$10.47 \pm 0.26$	$10252 \pm 47$	$-10.27 \pm 0.10$	$196.20 \pm 0.90$	10.5	$10.48 \pm 0.69$
DOP	$11.20 \pm 0.34$	$11143 \pm 62$	$-11.59 \pm 0.13$	$213.25 \pm 1.19$	10.5	$11.18 \pm 0.71$

<sup>a</sup> Cousins and Mackay (2000).

<sup>b</sup> EPA EPIsuite (2015a,b).

software. On the other hand, the Z-EHMC, with a  $\Delta H_{\text{vap}}(T_{298}) = 98.93 \pm 1.75 \text{ kJ mol}^{-1}$  had a vaporization enthalpy of almost  $10 \text{ kJ mol}^{-1}$  lower than its isomer and to our knowledge; it is the first report for this substance.

### 3.2. Estimation of the vapor pressure

Table 2 presents the  $P_L/\text{Pa}$  of target, control and reference substances for bibliographic and experimental data.

Fig. 1 shows the results obtained.

This linear behavior is represented by the following equation

$$\ln(P/\text{Pa})_{\text{calcd}} = (1.156 \pm 0.021) \ln(t_0/t_a) + (8.22 \pm 0.25) \quad R^2 = 0.9993 \quad (4)$$

For BBP, the latest experimental vapor pressure value obtained of  $2 \times 10^{-4} \text{ Pa}$  of Gobble et al. (2014), is in good agreement with the value reported in this work but is one order of magnitude lower than the reported by Howard et al. (1985). As observed in Table 2, the DOP vapor pressure reported by Gobble et al. (2014) is in good agreement with our result, within experimental error. Also the mono-esters FAME 16:0 and 18:0 correlated well with the bibliographic data (van Genderen et al., 2002; Chickos et al., 2004).

In this context, the E-EHMC vapor pressure obtained was  $1.8 \pm 0.1 \times 10^{-4} \text{ Pa}$  at 298.15 K. This value was almost one order of magnitude lower than  $1.8 \times 10^{-3} \text{ Pa}$  reported in EPIsuite-EPA (2015a,b).

The Z-EHMC vapor pressure was experimentally determined in this work and, as far as we know, this is the first report of this property. As was observed, its value of  $9.8 \pm 0.1 \times 10^{-4} \text{ Pa}$  at 298.15 K is almost five times bigger than E-EHMC one.

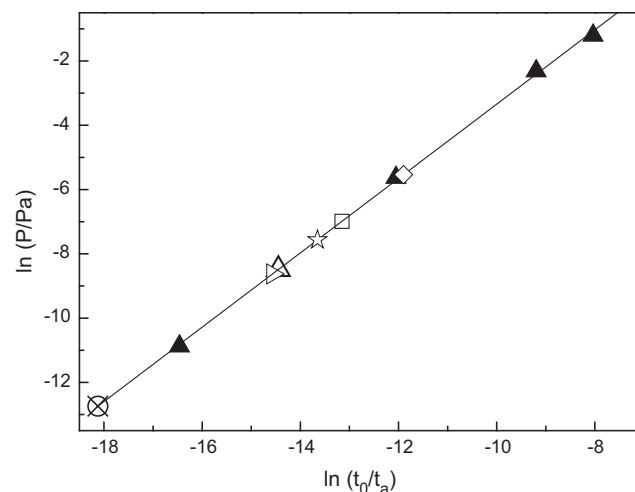


**Fig. 1.** Plot of  $\ln(P/\text{Pa})$  against  $\ln(t_0/t_a)$  of the references (▲) at  $T/K = 298.15$  (Table 2). The empty right triangle (▷), the empty star (☆), the empty triangle (△), the empty rhombus (◇), the empty square (□) and the cross circle (⊗) represents the value associated with BBP, Z-EHMC, E-EHMC, FAME 16:0, FAME 18:0 and DOP respectively calculated from the correlation.

As was well established, the energy necessary to promote evaporation of a liquid rises when the intermolecular forces of attraction increases at the condensed phase. In order to analyze these experimental aspects, DFT calculations were carried out to determine the dipole moment (in vacuum) of the molecules under study (Gaussian 09, Inc., Wallingford CT), (see computational details in Supplementary information S.7). A value of 2.84 D for E-EHMC was obtained while for Z-EHMC the value was 1.55 D. As was

**Table 4**  
Particle–gas partition coefficient,  $K_p$ , and the particle-bound fraction,  $\Phi$ %, estimated from the experimental  $P_L$  and  $K_{OA}$ .

	$\Delta H_{vap}$ (298 K) kJ mol <sup>-1</sup>	$\ln P_L$ Pa	$\log K_{OA}$	$P_L$		$K_{OA}$	
				$\log K_p$	$\Phi$ %	$\log K_p$	$\Phi$ %
Z-EHMC	98.93	-6.99	9.08	-2.059	16.43	-2.646	5.14
E-EHMC	108.91	-8.63	9.7	-1.447	41.31	-2.026	17.43
BBP	105.00	-8.484	9.66	-1.501	38.63	-2.066	16.23
DOP	126.56	-12.737	11.18	-0.087	94.96	-0.546	82.20

observed, the dipole moment molecular interaction for the Z-isomer should be lower than the E-one. The difference in the isomers dipole moment is consistent with the experimental results obtained for the vapor pressures and enthalpies of vaporization.

### 3.3. Estimation of octanol–air partition coefficients, $K_{OA}$

Table 3 summarizes the experimental and bibliographic data of  $K_{OA}$  regarding the reference and target substances. The intercepts and slopes reported in the table allow the estimation of  $K_{OA-GC}$  as a function of temperature.

These experimental measurements are very close to the ideal system behavior represented by a slope equal to 1 (see Figure N° S5.1 in supplementary information, S5). The uncertainty in the measured values is due mainly to the uncertainty introduced by the calibration procedure and it is not related to the measurement uncertainty of the retention times, which is generally very small.

From the bibliographic data available of  $K_{OA}$ , two members of the ubiquitous and widely used phthalate's family (Staples, 2003), BBP and DOP, have shown a different behavior. On the one hand, the  $\log K_{OA} = 8.7$  for BBP reported by van Genderen et al. (2002), did not correlate well with the standard calibration curve. Therefore, its experimental measure had been taken as unknown value (empty triangle in Figure N° S5.1) and the present result suggests a more accurate value of  $\log K_{OA} = 9.12 \pm 0.56$ .

For DEHP and DOP, a  $\log K_{OA} = 10.53$  had been suggested by Cousins and Mackay (2000) but an accurate value of  $11.18 \pm 0.71$  for DOP can be obtained from the present correlation (the cross circle, see Figure N° S5.1).

Furthermore, it was possible to determine a value of  $\log K_{OA} = 9.64 \pm 0.57$  for E-EHMC that agrees well with the EPA estimation of  $\log K_{OA} = 9.938$  at 298.15 K. Nevertheless, in the case of the Z-EHMC isomer, there is not reference in the literature. Then, its  $\log K_{OA} = 9.02 \pm 0.55$  is, to the best of our knowledge, the first report of this physico-chemical property at 298.15 K. See Table 3.

### 3.4. Estimating relevant atmospheric parameters for EHMCs and phthalates

#### 3.4.1. Determination of the gas–particle partition coefficient, $K_p$

In atmospheric sciences, gas–particle partitioning of SVOCs is commonly used to describe the global transport of airborne pollutants. The distribution of an organic substance between the gas phase and the surface of the airborne particles depends mainly on a combination of absorption and adsorption processes and can be described by an equilibrium constant named gas–particle partition coefficient,  $K_p$  (m<sup>3</sup> μg<sup>-1</sup>), that was defined by (Pankow, 1987, 1994):

$$K_p = \frac{F/TSP}{A} \quad (5)$$

where  $F$  (retained by filter) and  $A$  (retained by adsorbent) are the equilibrium particle-phase and the equilibrium gas-phase concentration of the compound (ng m<sup>-3</sup>), respectively. TSP is the total suspended particulates in air μg m<sup>-3</sup>.

3.4.1.1. Estimating  $K_p$  from vapor pressure,  $P_L$ /Pa. It was demonstrated that the vapor pressure is a good descriptor of gas–particle partitioning coefficient,  $K_p$  for adsorption and absorption processes (Pankow, 1987). Many equations have been used to calculate  $K_p$  values from  $P_L$ /Pa for several SVOCs classes, but no equation has been presented for Z-/E-EHMC or phthalate esters. Weschler et al. (2008) used the values for PAHs because they reasonably resemble phthalate esters, then the relationship reported by Naumova et al. (2003) based on over 1800 partition coefficients for PAHs measured outdoors and indoors in three US cities.

$$\log K_p = -0.860 \log P_L / \text{Pa} - 4.67 \quad (6)$$

The  $K_p$  ( $P_L$ ) values are summarized in Table 4. The low affinity of Z-EHMC with the particulate phase was observed in contrast with DOP. A similar  $\log K_p$  could be observed for E-EHMC and BBP with an intermediate tendency to remain in the gas phase.

3.4.1.2. Estimating  $K_p$  from  $K_{OA}$ .  $K_{OA}$  is an excellent descriptor of the air–particle partitioning process and can be used to predict  $K_p$  when the predominant distribution process is the absorption (Harner and Bidleman, 1998). An empirical relationship derived by Finizio et al. (1997) from field measurements of PAHs compounds has been used in this work:

$$K_p = 1.88 \times 10^{-12} \times K_{OA} \quad (7)$$

Table 4 shows the values of  $\log K_p$  ( $K_{OA}$ ) obtained for the target substances. Within these results, Z-EHMC and DOP showed the lower and higher affinity to the particulate. On the other hand, E-EHMC and BBP have similar affinity to the particulate but, essentially, they will found in the gas-phase. In these experimental estimations, it can be observed that, for each molecule, the  $K_p$  ( $K_{OA}$ ) is systematically lower than  $K_p$  ( $P_L$ /Pa) because they are based on PM<sub>2.5</sub> and TSP, respectively. The concentration of a substance in/on the particle,  $F$ , is expected to be somewhat larger for PM<sub>2.5</sub> than for TSP (Finlayson-Pitts and Pitts, 2000). It could be inferred that the  $K_p$  calculated using the vapor pressure is larger than the  $K_p$  calculated using  $K_{OA}$  model, see Table 4, (Weschler et al., 2008). Nevertheless, other factors may contribute to this difference between the two models. On the other hand, Xiao and Wania (2003) concluded that, at the present, the data available are too imprecise to judge which of the two descriptors is the more appropriate.

#### 3.4.2. Estimating particle-bound fraction, $\Phi$ %

The  $\Phi$ %, can be obtained using the following equation:

$$\Phi = \frac{F}{F+A} = \frac{K_p TSP}{1 + K_p TSP} \quad (8)$$

Lohmann and Lammel (2004) collected information of several works related to the atmospheric particulate monitoring and classified the TSP experimental values according to four categories: urban, suburban, background, and remote, assigning them values of 55, 22, 14 and 7.7 μg m<sup>-3</sup>, respectively. Taking into account these different scenarios, the  $\Phi$ % were calculated (Eq. (8)) using the  $K_p$  obtained from the two models described above. In all cases,

a TSP decrease produced an increase in the gas phase concentration of the substances under study (see Table 4 and Figure N° S6.1a and 6.1b in supplementary information).

The mean values of  $\Phi$ % of both models predicted that E-EHMC would be more strongly adsorbed to the particulate than Z-EHMC but both isomers would be present predominantly in the gas phase ( $\Phi$ /E-EHMC = 17–41% and  $\Phi$ /Z-EHMC = 5–16%). On the other hand, DOP would be predominantly in the particulate phase ( $\Phi$  = 82–95%) while BBP would be found in the gas phase ( $\Phi$  = 16–39%). These predictions of phthalates partitioning were in agreement with those reported by Blanchard et al. (2013) in which the particulate fraction of BBP was 14.2% in outdoor air of Paris (France) and also with the reported by Wang et al. (2008), in which the particulate fraction for BBP was 19% and 20% for urban and suburban Nanjing (China), respectively. Furthermore, in the Arctic zone, Xie et al. (2007) determined the  $\Phi_{\text{mean}}$  for DMP, DEP, DnBP, BBP and DEHP, with values of 3, 5, 33, 40 and 71, respectively. BBP also coincided with a reported result of 40%, within experimental error.

In the case of DOP, it was observed that its particulate-bound could vary from 25% up to 100% in the two measured scenarios (Wang et al., 2008). This could be attributed to TSP values the differences and to the non-equilibrium conditions in which partitioning between the gas and particulate phases of the atmosphere takes place in the outdoor. Nevertheless, taking into account the 71% reported for DEHP in the work of Xie et al. (2007), and considering that DOP has a lower vapor pressure and larger  $K_{\text{OA}}$  than DEHP, (Tables 2 and 3), it could be reasonable for a bound-particle of 82–95% for DOP, close to the 100%.

Mayol-Bracero et al. (2001) detected E-EHMC in 87% of organic aerosol samples and it was also detected in the atmosphere above the open sea but the concentrations were not reported. According to the present results, the EHMC delivered to the ecosystem, could be present in the atmosphere in both, the gas and particulate phase but the estimation of the particle-bound for E-EHMC (17–41%) and Z-EHMC (5–16%) suggested that both isomers should be mainly in the gas phase. Recently, Tsui et al. (2014) reported the presence of E-EHMC in the Arctic sea water and have proposed that this could be the result of atmospheric long-range or short-range transport (Wania and Mackay, 1996; Bennett et al., 2001). In this context, the occurrence of E-EHMC and Z-EHMC in the gas and particulate phase samples collected in Córdoba (Argentina) showed that both compounds are mainly in the gas phase. These experimental results should be in accordance with the present work (Chiappero et al., to be submitted).

#### 4. Conclusions

From these novel measurements arise a  $\Delta H_{\text{vap}}$  ( $T_{298}$ ) of  $108.91 \pm 1.82$  and  $98.93 \pm 1.75$  kJ mol<sup>-1</sup>, for E-EHMC and Z-EHMC, respectively. Additionally, it was proposed that the higher vapor pressure at 298.15 K of Z-EHMC is directly related to the decrease in the intrinsic dipole–dipole interactions of such molecules in condensed phase as compared to the corresponding E-EHMC isomer.

With a  $\log K_{\text{OA}}$  of  $9.64 \pm 0.57$  and  $9.02 \pm 0.55$  for E-EHMC and Z-EHMC, respectively, both semi-volatiles compounds are including in the range of  $6 < \log K_{\text{OA}} < 10$  so, their dry gaseous deposition on to vegetation and soil could be an efficient scavenging pathway from the atmosphere.

New values of  $\log K_{\text{OA}}$  for BBP,  $9.12 \pm 0.56$ , and DOP,  $11.18 \pm 0.71$ , have been proposed.

According to the present results, the EHMC released into the environment, could be present in the atmosphere in both, the gas and particulate phase. Nevertheless, their particle-bound fraction

estimation suggested that both isomers should be mainly in the gas phase.

#### Conflict of interest

The authors declare no competing financial interest.

#### Acknowledgment

This research was supported by ANPCyT-PRH N°20 (PICT103), CONICET (PIP569), SECyT\_UNMdP, SECyT\_UNRC.

M.S.C., H.A.M and C.N.P. are members of CONICET. C.N.P. thanks CONICET for graduate fellowship.

#### Appendix A. Supplementary material

Supplementary data associated with this article can be found, in the online version, at <http://dx.doi.org/10.1016/j.chemosphere.2015.07.035>.

#### References

- Balmer, M.E., Buser, H.-R., Muller, M.D., Poiger, T., 2005. Occurrence of some organic UV filters in wastewater in surface waters, and in fish from Swiss lakes. *Environ. Sci. Technol.* 39, 53–62.
- Bennett, D.H., Scheringer, M., McKone, T.E., Hungerbühler, K., 2001. Predicting long-range transport: a systematic evaluation of two multimedia transport models. *Environ. Sci. Technol.* 35, 181–189.
- Bidleman, T.F., 1984. Estimation of vapor pressure for nonpolar organic compounds by capillary gas chromatography. *Anal. Chem.* 8, 499–512.
- Blanchard, M., Teil, M.-J., Dargnat, C., Alliot, F., Chevreuil, M., 2013. Assessment of adult human exposure to phthalate esters in the Urban Centre of Paris (France). *Bull. Environ. Contam. Toxicol.* 90, 91–96.
- ChemSpider Database, 2015. <<http://www.chemspider.com>>. Data is Generated Using the EPA EPIsuite (accessed 22.01.15).
- ChemSpider Database, 2015. <<http://www.chemspider.com>>. Data is Generated Using the ACD/Labs' ACD/PhysChem Suite (accessed 22.01.15).
- Chickos, J.S., Hosseini, S., Hesse, D.G., 1995. Determination of vaporization enthalpies of simple organic molecules by correlations of changes in gas chromatographic net retention times. *Thermochim. Acta* 249, 41–62.
- Chickos, J.S., Zhao, H., Nichols, G., 2004. The vaporization enthalpies and vapor pressures of fatty acid methyl esters C18, C21 to C23, and C25 to C29 by correlation – gas chromatography. *Thermochim. Acta* 424, 111–121.
- Chickos, J., Lipkind, D., 2010. An examination of factors influencing the thermodynamics of correlation-gas chromatography as applied to large molecules and chiral separations. *J. Chem. Eng. Data* 55, 698–707.
- Clausen, P., Hansen, V., Gunnarsen, L., Afshari, A., Wolkoff, P., 2002. Emissions of phthalates from PVC flooring in two very different test chambers. In: Levin, H. (Ed.), *Indoor Air 2002: Proceedings of the 9th International Conference on Indoor Air Quality and Climate*, vol. 2. Santa Cruz, CA, pp. 932–937.
- Cousins, I., Mackay, D., 2000. Correlating the physical-chemical properties of phthalate esters using the 'three solubility' approach. *Chemosphere* 41, 1389–1399.
- Fent, K., Zenker, A., Rapp, M., 2010. Widespread occurrence of estrogenic UV-filters in aquatic ecosystems in Switzerland. *Environ. Pollut.* 158, 1817–1824.
- Finlayson-Pitts, B.J., Pitts, J.N., 2000. *Chemistry of the Upper and Lower Atmosphere*. Academic Press, San Diego.
- Finizio, A., Mackay, D., Bidleman, T., Harner, T., 1997. Octanol-air partition coefficient as a predictor of partitioning of semi-volatile organic chemicals to aerosols. *Atmos. Environ.* 31, 2289–2296.
- Giokas, D.L., Sakkas, V.A., Albanis, T.A., Lampropoulou, D.A., 2005. Determination of UV-filter residues in bathing waters by liquid chromatography UV-diode array and gas chromatography–mass spectrometry after micelles mediated extraction–solvent back extraction. *J. Chromatogr. A* 1077, 19–27.
- Gobble, C., Chickos, J., Verevkin, S.P., 2014. Vapor pressures and vaporization enthalpies of a series of dialkyl phthalates by correlation gas chromatography. *J. Chem. Eng. Data* 59, 1353–1365.
- Harner, T., Bidleman, T.F., 1998. Octanol-air partition coefficient for describing particle/gas partitioning of aromatic compounds in urban air. *Environ. Sci. Technol.* 32, 1494–1502.
- Hinckley, D.A., Bidleman, T.F., Foreman, W.T., Tuschall, J.R., 1990. Determination of vapor pressures for nonpolar and semipolar organic compounds from gas chromatographic retention data. *J. Chem. Eng. Data* 35, 232–237.
- Howard, P.H., Banerjee, S., Robillard, K.H., 1985. Measurement of water solubilities octanol/water partition coefficients and vapor pressures of commercial phthalate esters. *Environ. Toxicol. Chem.* 4, 653–661.
- Lohmann, R., Lammel, G., 2004. Adsorptive and absorptive contributions to the gas-particle partitioning of polycyclic aromatic hydrocarbons: state of knowledge

- and recommended parameterization for modeling. *Environ. Sci. Technol.* 38, 3793–3803.
- Mackay, D., Shiu, W.Y., Ma, K.C., Lee, C.L., 2006. *Physical–Chemical Properties and Environmental Fate for Organic Chemicals on CD-ROM*, 2nd ed. CRC Press, Taylor & Francis, Boca Raton, FL.
- MacManus-Spencer, L.A., Tse, M.L., Klein, J.L., Kracunas, A.E., 2011. Aqueous photolysis of organic ultraviolet filter chemical octyl methoxycinnamate. *Environ. Sci. Technol.* 45, 3931–3937.
- Magi, E., Scapolla, C., Di Carro, M., Rivaro, P., Nguyen, K.T.N., 2013. Emerging pollutants in aquatic environments: monitoring of UV filters in urban wastewater treatment plants. *Anal. Methods* 5, 428–433.
- Mayol-Bracero, O.L., Rosario, O., Corrigan, C.E., Morales, R., Torres, I., Perez, V., 2001. Chemical characterization of submicron organic aerosols in the tropical trade winds of the Caribbean using gas chromatography/mass spectrometry. *Atmos. Environ.* 35, 1735–1745.
- Naumova, Y.Y., Offenber, J.H., Eisenreich, S.J., Meng, Q., Polidori, A., Turpin, B.J., Weisel, C.P., Morandi, M.T., Colome, S.D., Stock, T.H., Winer, A.M., Alimokhtari, S., Kwon, J., Maberti, S., Shendell, D., Jones, J., Farrar, C., 2003. Gas/particle distribution of polycyclic aromatic hydrocarbons in coupled outdoor/indoor atmospheres. *Atmos. Environ.* 37, 703–719.
- Odabasi, M., Cetin, E., Sofuoglu, A., 2006. Determination of octanol–air partition coefficients and supercooled liquid vapor pressures of PAHs as a function of temperature: application to gas–particle partitioning in an urban atmosphere. *Atmos. Environ.* 40(34), 6615–6625.
- Odabasi, M., Cetin, B., 2012. Determination of octanol–air partition coefficients of organochlorine pesticides (OCPs) as a function of temperature: application to air–soil exchange. *J. Environ. Manage.* 113, 432–439.
- Pankow, J.F., 1987. Review and comparative analysis of the theories of partitioning between the gas and aerosol particulate phases in the atmosphere. *Atmos. Environ.* 21, 2275–2283.
- Pankow, J.F., 1994. An absorption model of gas–particle partitioning of organic compounds in the atmosphere. *Atmos. Environ.* 28, 185–188.
- Pattanaargson, S., Munhapol, T., Hirunsupachot, P., Luangthongaram, P., 2004. Photoisomerization of octyl methoxycinnamate. *J. Photochem. Photobiol., A* 161, 269–274.
- Perry, E.S., Weber, W.H., 1949. Vapor pressure of phlegmatic liquids. II high molecular weight esters and silicon oils. *J. Am. Chem. Soc.* 71, 3726–3730.
- Radonic, J., Vojinovic, P., Miloradov, M., Turk Sekulic, M., Kiurski, J., Djogo, M., Milovanovic, D., 2011. The octanol–air partition coefficient,  $K_{OA}$ , as a predictor of gas–particle partitioning of polycyclic aromatic hydrocarbons and polychlorinated biphenyls at industrial and urban sites. *J. Serb. Chem. Soc.* 76, 447–458.
- Richardson, S.D., 2010. Environmental mass spectrometry: emerging contaminants and current issues. *Anal. Chem.* 82, 4742–4774.
- Rohac, V., Musgrove, J.E., Ruzicka, K., Ruzicka, V., Zabransky, M., Aim, K., 1999. Thermodynamic properties of di-methylphthalate along the (vapour + liquid) saturation curve. *J. Chem. Thermodyn.* 31, 971–986.
- Rohac, V., Ruzicka, K., Ruzicka, V., Zaitsau, D.H., Kabo, G.J., Diky, V., Aim, K., 2004. Vapour pressure of diethyl phthalate. *J. Chem. Thermodyn.* 36, 929–937.
- Schlumpf, M., Durrer, S., Faass, O., Ehnes, C., Fuetsch, M., Gaille, C., Henseler, M., Hofkamp, L., Maerkel, K., Reolon, S., Timms, B., Tresguerres, J.A.F., Lichtensteiger, W., 2008. Developmental toxicity of UV filters and environmental exposure: a review. *Int. J. Androl.* 31, 144–151.
- Shoeib, M., Harner, T., 2002. Using measured octanol–air partition coefficients to explain environmental partitioning of organochlorine pesticides. *Environ. Toxicol. Chem.* 21, 984–990.
- Small, P.A., Small, K.W., Cowley, P., 1948. The vapor pressures of some high boiling esters. *Trans. Faraday Soc.* 44, 810–816.
- Staples, C.A., Peterson, D.R., Parkerton, T.F., Adams, W.J., 1997. The environmental fate of phthalate esters: a literature review. *Chemosphere* 35, 667–749.
- Staples, C.A., 2003. *The Handbook of Environmental Chemistry*, vol. 3, Part Q, 1–347. Springer <http://dx.doi.org/10.1007/b11460>.
- Stephenson, R.M., Malanowski, S., 1987. *Handbook of the Thermodynamics of Organic Compounds*. Elsevier, New York.
- Tsui, M.M., Leung, H.W., Wai, T.C., Yamashita, N., Taniyasu, S., Liu, W., Lam, P.K.S., Murphy, M.B., 2014. Occurrence, distribution and ecological risk assessment of multiple classes of UV filters in surface waters from different countries. *Water Res.* 67, 55–65.
- van Genderen, A.C.G., van Miltenburg, J.C., Blok, J.G., van Bommel, M.J., van Ekeren, P.J., van den Berg, G.J.K., Oonk, H.J., 2002. Liquid–vapour equilibria of the methyl esters of alkanolic acids: vapour pressures as a function of temperature and standard thermodynamic function changes. *Fluid Phase Equilibria* 202, 109–120.
- Wang, P., Wang, S.L., Fan, C.Q., 2008. Atmospheric distribution of particulate- and gas-phase phthalic esters (PAEs) in a Metropolitan City, Nanjing, East China. *Chemosphere* 72, 1567–1572.
- Wania, F., Lei, Y.D., Harner, T., 2002. Estimating octanol–air partition coefficients of nonpolar semivolatile organic compounds from gas chromatographic retention times. *Anal. Chem.* 74, 3476–3483.
- Wania, F., Mackay, D., 1996. Tracking the distribution of persistent organic pollutants. *Environ. Sci. Technol.* 30, 390A–396A.
- Wania, F., McLachlan, M.S., 2001. Estimating the influence of forests on the overall fate of semivolatile organic compounds using a multimedia fate model. *Environ. Sci. Technol.* 35, 582–590.
- Weschler, C.J., Salthammer, T., Fromme, H., 2008. Partitioning of phthalates among the gas phase, airborne particles and settled dust in indoor environments. *Atmos. Environ.* 42, 1449–1460.
- Xiao, H., Wania, F., 2003. Is vapor pressure or the octanol–air partition coefficient a better descriptor of the partitioning between gas phase and organic matter? *Atmos. Environ.* 37, 2867–2878.
- Xie, Z., Ebinghaus, R., Temme, C., Lohmann, R., Caba, A., Ruck, W., 2007. Occurrence and Air–Sea Exchange of Phthalates in the Arctic. *Environ. Sci. Technol.* 41, 4555–4560.
- Zenker, A., Schmutz, H., Fent, K., 2008. Simultaneous trace determination of nine organic UV-absorbing compounds (UV filters) in environmental samples. *J. Chromatogr. A* 1202, 64–74.